PROGRESS IN APPLIED SCIENCE AND TECHNOLOGY
Faculty of Science and Technology
Rajamangala University of Technology Thanyaburi
Prog Appl Sci Tech. 2022; 12(1):23-35
ISSN (Print): 2730-3012
ISSN (Online): 2730-3020
https://ph02.tci-thaijo.org/index.php/past

Research Article

Received: February 06, 2022
Revised: April 01, 2022
Accepted: April 13, 2022

DOI: 10.14456/x0xx00000x

Surface Modification of Plant-Drive Calotropis Gigantea Fiber Reinforced Polypropylene Composites

Haydar U. Zaman* and Ruhul A. Khan
Institute of Radiation and Polymer Technology, Bangladesh Atomic Energy Commission, P.O. Box 3787, Savar, Dhaka, Bangladesh
*E-mail: haydarzaman07@gmail.com

Abstract

In the present study, calotropis gigantea fiber (CGF)/polypropylene (PP) composites with four different weight percentages of CGFs (10, 20, 30, and 40%) were made by compression molding using the film stacking method. The CGF content in the composites was optimized and 40 wt% CGF content exhibited the best mechanical properties. Composites containing 40% of CGF improved tensile modulus and impact strength by 256.2% and 94%, respectively in comparison to virgin PP but achieved 41.8% at 30% CGF content in tensile strength. In our current work, the CGF surface was modified by alkaline treatment (ACGF), and alkaline pretreated CGF was modified with two types of silane coupling agents such as aminopropyltrimethoxy silane (AS) and tetramethoxyorthosilicate (TS) to improve the mechanical performance of PP/CGF composite. For PP/CGF composites, adding silane after alkali pretreatment improves the mechanical properties and subsequently the water absorption of the composites. This tendency has become further noticeable with the growth of CGF content. In this article the maximum mechanical properties of PP/ACGF/TS composites were achieved in 40 wt% CGF content, which showed 19.1% tensile modulus and 67.9% impact strength compared to PP/CGF composites but achieved 24.3% in 30% CGF content in tensile strength. The water absorption test showed that PP/ACGF/TS composites exhibit less water absorption than both PP/ACGF/AS and PP/CGF composites. The CGF surface morphologies and the fractured surfaces of the composites show an improvement in the interfacial CGF-PP adhesion of reinforced composites with alkali-pretreated silane-treated CGFs. The addition of magnesium hydroxide to PP/ACGF/AS and PP/ACGF/TS significantly reduced the horizontal combustion rate. DSC results showed that the addition of AS and TS for CGF resulted in higher crystallization, melting and crystallinity of the composites. The thermal stability of PP/ACGF/TS composite was higher than PP/ACGF/AS and higher than PP/ACGF composite.

Keywords: Composites, Polypropylene, Calotropis Gigantea Fiber, Silane, Mechanical and Thermal Properties

1. Introduction

Lately, interest in composites made of natural fibers (NFs) has increased significantly (1-5). At present, NFs such as vetiver, calotropis gigantea, abaca, snake grass, etc. are extensively used to make a composite due to their high toughness, high specific properties, lightweight, recyclability, low price, and "eco-friendly" (6, 7). These fibers are instinctively incompatible with hydrophobic thermoplastics. Plant fibers reinforced thermoplastic composites are gaining attractiveness with some imperfections in industrial packaging and performances for sheet work, fences, furniture, and construction (8, 9).

Various wide research work on NF composites conducted by Haydar and colleagues has established that NFs are a great alternative to synthetics (10-13).

Plant-drive NF is calotropis gigantea fiber (CGF). We chose CGF because it has sufficient buoyancy, hydrophobic-oleophilic features, high oil absorption capacity, and oil-water separation efficiency and is used as an oil-absorbing ingredient in the oil separation process to remove oil from water. CGF belongs to the family of Asclepiadaceae and lives in China, India, Bangladesh, and various portions of the world. This tree grows up to 3-5 m in height and forms waxy flowers in clusters. Furthermore, it has oval-shaped pale green leaves and stalks with a milky nature, which is further enriched by fibers. The fibers obtained from the stems of the CG plant are used for composite production. Extract CG bark fiber contains 73.8% cellulose, 20.5% hemicellulose, 2.7% lignin, and 1.18% waxy substances (14). When selecting new fibers, chemical elements performance a vital role in determining the mechanical features of the fiber in the NF composite. Table 1 lists the chemical components of NFs that are already used as reinforcements in NF composites with CG fibers. Although cellulose fibers have multiple benefits, cellulose fibers reduce the adverse effects of high temperatures and the ubiquity of moisture absorption. Hydroxyl groups represent cellulose to form different hydrogen bonds and CGFs to form hydrophilic. Manufactured composites, including nonpolar (hydrophobic) thermoplastic matrix and polar (hydrophilic) NFs, reduce mechanical features due to weaknesses in the plastic material and fiber (15).

Composites using CGF as a reinforcing fiber in the thermosetting resin matrix have received considerable attention from scientists around the world for the potential for evolving plants (16, 17). Thermoplastic composites have several benefits over thermoset composites. Some of them are higher fracture strength, better solvent resistance, reusability, and quick, fresh and automatic processing (18). The key fascination of thermoplastic composites is the possibility of destruction in a very short time as no chemical reaction is essential. Adding NF to the matrix causes significant variations in the mechanical properties of the composite. The contents of the filler, the size of the filler, and the degree of the filler-matrix interfacial bond, determine the physical properties of the composite and the reasons for the improvement of mechanical strength (19). So, the right choice of fillers for a specific matrix is a vital issue in improving filler-matrix interface adhesion.

In this study, PP was selected as a thermoplastic resin because it has several outstanding features such as transparency, superior surface strength, high impact strength, high heat distortion temperature, and dimensional stability. PP is moreover very fit for filling, strengthening, and mixing. PP has a high melting point (160°C-170°C) and softening point (above 149°C), and hardness comparatively higher than other available thermoplastics. It contains a rare combination of excellent physical, mechanical, thermal, electrical, and chemical features. Due to the excellent adjustment of respectable thermal features, low humidity pickup, and respectable dielectric features, it is a great ingredient for electrical applications. The most promising way to make PP composite with fibrous natural polymer from biomass source (20-22). NFs are hydrophilic whereas synthetic polymers are hydrophobic (23). Poor bonding between the NF and the matrix frequently prevents NFs from acting as fillers, followed by poor distribution, insufficient strength, and low mechanical features (24, 25). Thus, the coupling agent must be incorporated or chemically modified for the final application of the composite components of NFs. One of the most effective ways to develop the physical properties of composites is through chemical treatments. The chemicals can interact effectively with cellulose and activate the hydroxyl group, which can induce the necessary features of the polymer. Alkali pre-treatment and consequent silane treatment were used to improve the bond between these two differing surfaces (26). This can be attained by pre-treatment by changing the surface topology or selecting the right component of the bonding system. Improvements in the mechanical properties of the composite as a result of NF surface changes have been reported by several workers (27-30). An extensive literature review has revealed that alkali pretreated CGF reinforcement PP-based AS and TS-treated composites have not yet been released. In the present work, the CGF-reinforced PP composites were prepared and the properties were examined. The CGF content was varied from 0-40 wt% and its effects on tensile strength, tensile modulus, impact strength and water absorption properties were measured. CGFs

were treated with alkali-pretreated two silane treatments; aminopropyltrimethoxy silane (AS) and tetramethoxyorthosilicate (TS), in order to develop adhesion between the CGF and the PP matrix. The effects of alkali-pretreated silane treatments on mechanical, water absorption, and thermal features of the CGF-reinforced PP composites were examined. CGF surface morphology and fractured surfaces of untreated and treated PP/CGF composites were investigated by scanning electron microscopy (SEM) providing the information for the evaluation of interfacial CGF-PP adhesion.

2. Experimental

2.1 Materials

The plant calotropis gigantea has been collected from purra village in the Manikganj district of the Dhaka division in Bangladesh. The detergent as a liquid was obtained from Chennai, India. CGF's diameter was ~ 0.22 ± 0.055 mm. Isotactic PP (M110) matrix component with 0.9 g/cc and MFI 11g/10 min was obtained from M/s Haldia Petrochemicals, Calcutta, India. Aminopropyltrimethoxy silane (AS, 97%) and tetramethoxyorthosilicate (TS, 99%) were obtained from E. Merck, Darmstadt, Germany, and used for chemical treatment. Magnesium hydroxide ($Mg(OH)_2$) as a flame retardant was obtained from Sigma-Aldrich and other chemicals, namely pure methanol and NaOH were purchased from Aldrich Chemical Co. Inc. (USA).

2.2 Methods

A CG plant older than one year seems to be quite suitable for fiber extraction. The leaves, including the stalks, were cut off from the tree and the stems were cut to the required length. It was then dried for three days at room temperature and then the steams were extracted by hand decorticated method. The CG plant and the extracted fibers are displayed in Figure 1. The characteristics of CG fiber were given in Table 1. Unwanted ingredients were separated from the CGF. Then cut the same size 140 mm. Well-drained CGFs were washed for 1 hour with washing detergent solution (2%) and then rinsed with pure water to remove foreign components. The fibers were dried at 60°C for 24 h to adjust humidity (1-2%) and then placed in a vacuum desiccator. The prepared sample was weighed by analytical electrical balance.

Figure 1 Extraction of CGF: (a) CG plant, (b) extracted CGF

Table 1 Features of CG fiber

Description	values
Physical properties	
Density (g/cc)	1.360
Diameter (μm)	90-260
Chemical compositions	
Cellulose (%)	73.8
Hemicellulose (%)	20.5
Lignin (%)	2.7
A Wax (%)	1.18
Mechanical properties	
Tensile strength (N)	7.95
Percentage of elongation (%)	5.03

2.2.1 Pretreatment of CG fibers

Washed and dried CGFs were placed in a tray. A 5% alkali solution was added to a tray and the CGFs were immersed in this solution at room temperature for about 1 hour. Then, all NaOHs were excluded until they were washed in pure water until a more alkaline reaction of the water was indicated. The final laundry was then complete with 3% acetic acid to deactivate the last drops of NaOH.

2.2.2 Chemical treatments

Alkaline pre-treated CGFs were chemically treated with aminopropyltrimethoxy silane (AS) and tetramethoxyorthosilicate (TS). A 3 wt% solution of silane was made by mixing AS or TS in a mixture of methanol/water (50:50) for 1 hour. Alkaline pre-treated CGFs were immersed in this solution for 1 h at room temperature. After the coupling reaction was over, the CGFs were dehydrated at 70°C and placed in a vacuity oven for 30 h at a constant weight.

2.2.3 Preparation of composites

The dried CGFs were lined up in parallel arrangement, glued with adhesive tape, and molded between PP sheets (0.25-0.30 mm

thickness). Both untreated and treated CGF (10-40 wt%) composites were fabricated using a hot press machine by film stacking method. Composites were manufactured by pressing this stacking at 180°C for 5 min under the constant pressure of 10 MPa. After that, the mold was removed from the press, then securely stuck between the two steel mold plates, and the last one was quickly extinguished by ice water. The diagram of the fabricated composite is displayed in Figure 2. Compositions of control and modified CGF/PP composites are shown in Table 2.

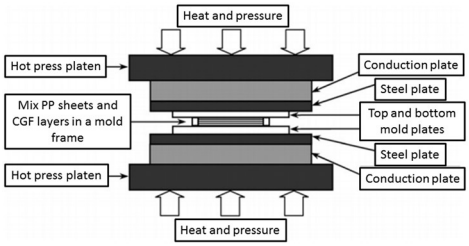

Figure 2 Schematic representation of the hot press used to fabricate composite plates.

Table 2 Compositions of control and modified CGF/PP composites.

I (wt%)	Sample designation			
	A	**B**	**C**	**D**
PP	100	100	100	100
CGF	0, 10, 20, 30, 40	–	–	–
ACGF	–	0, 10, 20, 30, 40	–	–
AACGF	–	–	0, 10, 20, 30, 40	–
TACGF		–	–	0, 10, 20, 30, 40
I (phr)	A1	B1	C1	D1
PP	100	100	100	100
CGF	0, 40	–	–	–
ACGF	–	0,40	–	–
AACGF	–	–	0, 40	–
TACGF	–	–	–	0,40
$Mg(OH)_2$	10	10	10	10

I: Ingredients; A; PP/CGF; B: PP/ACGF; C: PP/ACGF/AS; D: PP/ACGF/TS; A1: PP/CGF/FR; B1: PP/ACGF/FR; C1: PP/ACGF/AS/FR; D1: PP/ACGF/TS/FR; ACGF: Alkalized CGF; AACGF: AS treated ACGF; TACGF: TS treated ACGF

2.2.4 Mechanical measurement of composites

Tensile measurements for composites using a Shimadzu UTM (model AG-1, Japan) by ASTM-D 638-03 were performed at a crosshead speed of 10 mm/min and a gauge length of 20 mm. Izod Impact test was performed with an impact machine (model, Toyo Seiki Co., Japan) according to ASTM-D 256. The dimensions of a sample for impact testing were 63.5 mm × 3 mm × 12.7 mm. The hardness of the composites was measured using a Rockwell Hardness Testing Machine according to ASTM D 785-98 (31) on the Rockwell L scale. All tests were conditioned at room temperature (27°C ± 3°C) and relative humidity at 50 ± 3%. The reported values averaged five measurements.

2.2.5 Morphological properties

The morphology of the tensile fracture surface of untreated and treated composites was observed under a scanning electron microscope (SEM, model JEOL JSM-5310) at 20 kV. Prior to SEM, samples were coated with a thin layer of gold (25 nm) under vacuum using a BALTEC SCD 050 sputter coater layer to avoid accumulation of electrical charge.

2.2.6 Flammability test

Sample combustion was detected by a horizontal combustion test using ASTM D635 using a horizontal-vertical flame chamber instrument (Atlas, HVUL). In the horizontal flame test, the sample was placed horizontally and a fire ignited by natural gas was applied to one end of the sample. Combustion rate was deliberated from the following countenance (2.1):

$$B_r = \frac{60\ell}{t} \quad (2.1)$$

where B_r is the combustion rate in mm/min, ℓ is the length of the burn travel and t is the time in seconds for burn travel. A minimum of five measurements were recorded in each specimen.

2.2.7 Thermal properties

The thermal properties of composites (crystallization temperature, T_c, melting temperature, T_m, melting enthalpy, ΔH_m) were measured with a DSC (DSC, Perkin Elmer DSC-7). A specimen was placed in an aluminum pan and each specimen (5-10 mg) was heated from 30°C to 250°C at a heating rate of 10°C/min and then held at 250°C to confirm a duplicate thermal history. The T_c, T_m, ΔH_m, and crystallinity (X_c) were measured from the first heating scan. X_c

was deliberated from the following countenance (2.2):

$$X_c(\%) = \frac{\Delta H_m}{\Delta H_{m(crys)}} \times 100 \quad (2.2)$$

where ΔH_m is the melting enthalpy of a specimen and it is the melting enthalpy of 100% crystal PP (138 J/g) (32). The thermal degradation of composites was measured with a Perkin Elmer Thermogravimetric analyzer (TGA; Waltham, Massachusetts, USA) under the following conditions: 5–10 mg of specimens, a heating rate of 20°C/min, temperature range of 25–600°C and air flow rate of 20 mL/min.

2.2.8 Water absorption evaluation

Untreated and treated PP/CGF composites were applied for water absorption. Specimens were dried at 70°C and removed from the water periodically until they reach a constant weight before being immersed in distilled water at 25°C. The surface water of the specimens was wiped with a clean cloth and then the specimens were weighed. The water absorption was measured as follows:

$$\text{Water absorption } (\%) = \frac{W_2 - W_1}{W_1} \times 100$$

where W_2 and W_1 are the weight of the specimen after and before soaking, respectively.

3. Results and Discussion

3.1 Tensile properties

Figure 3(A) shows the tensile strength of control and treated PP/CGF composite samples against CGF content. It can be seen that the tensile strength of PP/CGF composite gradually increases with increasing CGF content up to 30 wt% and then decreases with CGF content. According to other researchers (11, 33), the tensile strength increases with CGF content. This behavior is largely recognized for the transfer of even stress from the matrix to the fiber. At low filler concentration (10 wt%), composites exhibit poor tensile properties due to low CGF content, low CGF population, and low load transfer capacity with each other. Consequently, tension is deposited at definite points in the composites, and extremely limited strains happen in the PP. At 30 wt% CGF loading level, the CGF population is optimal for the highest adaptation and the fiber energetically participates in tension transfer. Due to the higher filler loading (40 wt%), inferior adhesion between CGF and PP, the composite exhibits weak tensile properties. At this stage, the fiber agglomeration in the PP matrix leads to non-uniform stress transfer and eventually leads to microcrack formation, resulting in a poor interfacial bond between PP and CGF.

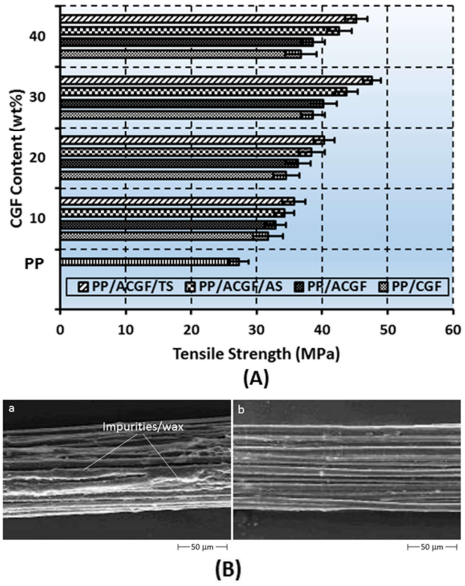

Figure 3 (A) Tensile strength of PP/CGF, PP/ACGF, PP/ACGF/AS, and PP/ACGF/TS composite samples; and (B) SEM micrographs of (a) untreated and (b) alkali-treated CGF.

The correlation between tensile strength and CGF content with and without alkali pretreated silane treatment is shown in Figure 3(A). It was found that the tensile strength of PP/ACGF, PP/ACGF/AS, and PP/ACGF/TS composites increased by 4%, 12.9%, and 24.3%, respectively, compared to the 30 wt% CGF/PP composite. For PP/ACGF sample, CGF was responsible for increased tensile strength to remove natural and synthetic impurities (such as lignin, hemicellulose, and wax & oils) that covered the external surface of the fiber cell wall and improves microporosity with plenty of holes and cavities on the surface. SEM image (Figure 3B, a) on the surface of untreated CGF bundles indicates the presence of oil, wax and surface impurities. Wax and oil deliver a shielding layer to the surface of the CGFs but they contribute to the bonding of futile CGF-PP composites (34).

Figure 3 (B, b) shows the cleaner, and the fiber bundles are further separated with a higher serrated surface. This is perhaps due to the removal of the outer surface layer of the fiber by dissolving it in a chemical solution (NaOH) at the treatment stage. As a result, fibrillation can promote better mechanical interlocking. Mercerization grows the number of potentially reactive sites and permits better fiber soaking. In addition, mercerization decreases the diameter of the fiber, growing the shape ratio which leads to the improvement of irregular surface structure which improves the fine fiber-matrix interface bond and mechanical features (35).

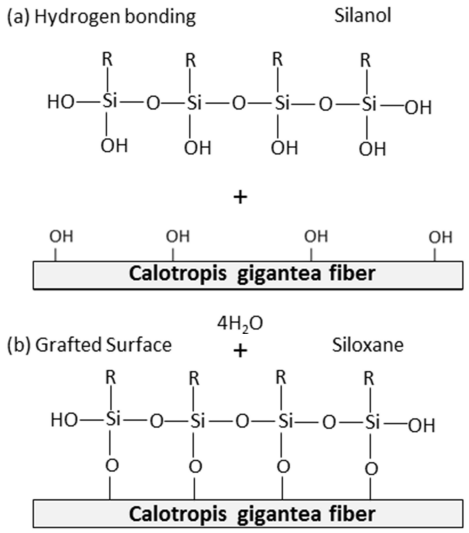

Figure 4 Bonding between silane and calotropis gigantea fibers: (a) hydrogen bonding; (b) the grafted surface.

As CGF load levels increased by 10 to 30 wt%, the tensile strength of alkaline pretreated silane (3 wt% AS or TS) treated CGF/PP composites increased significantly, and the tensile strength increased by 12.9% and 24.3%, respectively, compared to the 30 wt% PP/CGF composites. Firstly, enhanced tensile strength may be linked to hemicellulose and CGF extraction through alkali pretreatment, which alters the surface properties of CGF. Secondly, through silanization, silanol formation by hydrolysis of silane, condensation between silanols, and the creation of bonds between siloxane and CGF can be achieved consistently (Figure 4(a) and 4(b)). It has been speculated that silane action can create an easy distribution of PP in CGF, growth processability, and reduce CGF loss by shear force during composite processing. The four methoxy groups of TS can generate silanol by hydrolysis, whereas the three methoxy groups of AS can generate silanol by hydrolysis. Therefore, TS can generate a stronger silane crystal complex with CGF than AS. Furthermore, the aminopropyl group of AS may be more hydrophilic than that of TS. So, TS has better compatibility with PP than AS. It demonstrates the efficiency of silane action in increasing CGF/PP bonds, which has increased the tensile strength of the composite.

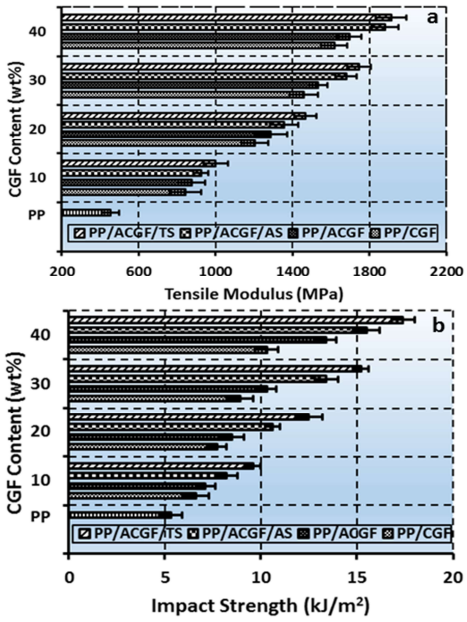

Figure 5 (a) Tensile modulus and (b) impact strength of PP/CGF, PP/ACGF, PP/ACGF/AS, and PP/ACGF/TS composites.

The correlation between tensile modulus and CGF content with and without alkali pretreated silane treatment is shown in Figure 5(a). It was observed that the tensile modulus of PP/CGF, PP/ACGF, P/ACGF/AS, and PP/ACGF/TS composites increased by 256.2, 272.4, 313.1, and 320.2% at 40 wt% CGF content, respectively, compared to virgin PP.

The tensile modulus has been developed with CGF content (36, 37). The growth in tensile modulus can be further closely correlated to the growth in the stiffness of the composite due to the CGF content (38). Treated composites (PP/ACGF, PP/ACGF/AS, and

PP/ACGF/TS) have higher tensile modulus than control composites. It was found that the tensile modulus of PP/ACGF, PP/ACGF/AS, and PP/ACGF/TS composites increased by 4.8%, 16.3%, and 19.1% in the 40 wt% CGF content, respectively, compared to the control sample. It has been observed that PP/ACGF/TS composites show better tensile modulus than other composites because there are some strong chemical bonds between the hydrophobic part of the silane of the CGF surface and PP.

3.2 Impact properties

Figure 5(b) shows the effect of PP/CGF composite on the Izod impact strength as a result of three treatments. At 40 wt% CGF loading level, the impact strength of PP/ACGF, PP/ACGF/AS, and PP/ACGF/TS composites was 30.1%, 50.5%, and 67.9% higher than PP/CGF composites. These outcomes are true that CGF was able to absorb energy because there was a strong interfacial bond between CGF and PP. As the CGF content increases, a greater force is essential to extract the CGF shots. This in turn increases the impact strength. The treated composites were higher impact strength values compared to the control sample. Higher impact strength for PP/ACGF/AS and PP/ACGF/TS composites was due to the optimal interaction between the treated CGF and PP matrix. CGF pullout and fiber agglomeration can be responsible for the low impact strength of the control sample.

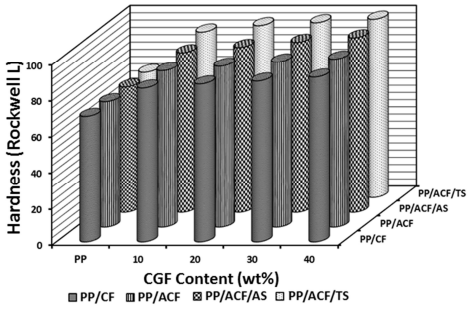

Figure 6 Hardness of PP/CGF, PP/ACGF, PP/ACGF/AS, and PP/ACGF/TS composites.

3.3 Rockwell hardness properties

The influence of CGF content on the Rockwell hardness of PP/CGF, PP/ACGF, PP/ACGF/AS, and PP/ACGF/TS composites is illustrated in Figure 6. In general, modulus-enhancing fibers of composites increase the hardness of their thermoplastics. As hardness is a function of fiber volume and modulus. The hardness of both controlled and treated composites has been observed to increase with increasing CGF content. The addition of CGF to PP decreased the flexibility of the PP chain in inelastic composites. At loading levels of 40 wt% CGF content, the hardness of PP/ACGF, PP/ACGF/AS, and PP/ACGF/TS composites was 2.1%, 6.2%, and 8.3% greater than PP/CGF composites. This results in better dispersion of CGF in PP which reduces the gaps and there is strong intrinsic adherence between PP and CGF.

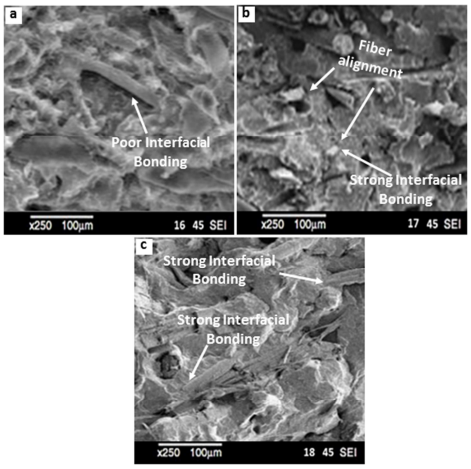

Figure 7 SEM micrographs of (a) PP/CGF (b) PP/ACGF/AS and (c) PP/ACGF/TS composites in 40 wt% CGF content.

3.4 Morphology of fractured surfaces

Figure 7(a-c) displays the tensile fracture surfaces of PP/CGF, PP/ACGF/AS, and PP/ACGF/TS composites in 40% CGF content, respectively. For PP/CGF composites (Figure 7, a), they appear to be isolated from the PP matrix and have a relatively large pull-out compared to other treated composites. These features propose fiber-to-fiber contact and poor interfacial bonding between CGF and PP. The interface construction of this composite cannot efficiently stress transfer. This statement agrees with the low tensile strength reported in Figure 3(A). We can see from Figure 7(b) that the CGFs was somewhat pulled out throughout the fracture process and maximum PP was attached to the surface of the CGFs. The fiber pullout of PP/ACGF/AS composite seems to be less than that of PP/CGF composite. This outcome has established a fine interface bond between CGF

and PP. For PP/ACGF/TS composites, CGFs were dismantled during the fracture process without a complete pull-out, and many PPs still stick to the surface of the CGF. This result has established that the interface bond between CGF and PP is much more favorable for PP/ACGF/TS composites than for PP/ACGF/AS composites.

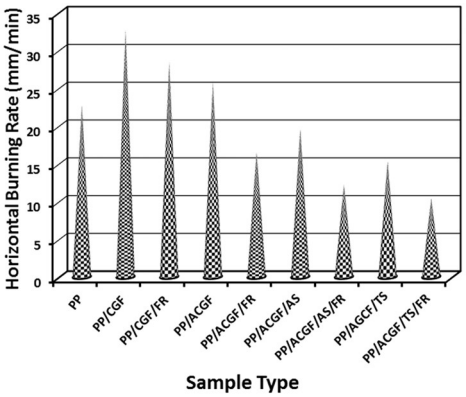

Figure 8 The combustion rate of virgin PP and its composite with and without fire resistance.

3.5 Flammability of the composites

The combustion rate of PP and its composites (control and treatment samples) with and without flame resistance is shown in Figure 8. It was experiential that PP/CGF composite exhibits a higher combustion rate than PP, which displays greater susceptibility to CGF flame. It can be said that $Mg(OH)_2$ acts as a fire-resistant for plastics and has been effective for high loads (39). But adding 10 wt% $Mg(OH)_2$ reduces the combustion rate of PP/CGF/FR composite to 13.3 wt%. This ensures that $Mg(OH)_2$ acts as a fire-resistant additive and releases substantial quantities of water at high temperatures thus diluting the quantity of fuel available to maintain combustion during a fire. Moreover, it is presumed that fire-resistant additive exploits heat from the ignition zone, declining the possibility of continuous ignition and producing a char through ignition after more fire-resistant protection and less smoke production. When 10% $Mg(OH)_2$ was incorporated with PP/ACGF/AS and PP/ACGF/TS composites separately, its flame retardant features were significantly enhanced. It was found that PP/ACGF/AS composite showed a moderate burning rate of 12.2 mm/min while PP/ACGF/TS composite exhibited incredible progress in the fire retardancy having a burning speed of about 10.4 mm/min. Thus, the results suggested that the addition of fire retardant improved the flame resistance property of the silane-treated composites.

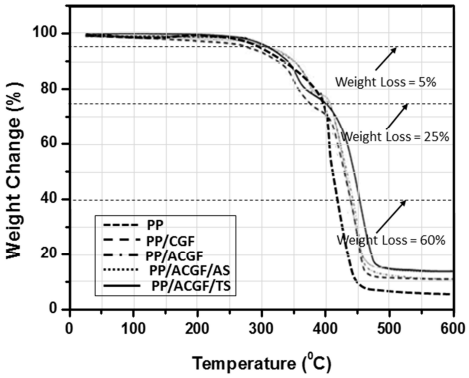

Figure 9 TGA thermograms of virgin PP, PP/CGF, PP/ACGF, PP/ACGF/AS, and PP/ACGF/TS composites.

3.6 Thermogravimetric analysis (TGA)

The TGA curves of virgin PP, PP/CGF, PP/ACGF, PP/ACGF/AS, and PP/ACGF/TS composite samples are presented in Figure 9. The decay temperatures of virgin PP and its composites are listed in Table 3. For instance, the primary decaying temperature (T_{onset}) is shown in Figure 9 and Table 3 displays that the T_{onset} increased from 251.3°C for virgin PP to 277.2°C for PP/CGF composite with a char residue of 10.8 wt%, which indicates that the thermal stability of PP was improved. It has also been observed that in a one-step degradation process from 251.3°C to 451.3°C, the weight of the virgin PP decreases, after which a very small amount of PP residue remains in the gaseous products due to the thermal degradation of the PP at high temperatures (40). For PP/ACGF composite, the T_{onset} was about 34.1°C better than PP as shown in Table 3. However, in the case of PPF/ACGF/AS and PP/ACGF/TS composites, a two-stage degradation process has been observed where weight loss at 260.2°C coincides with CGF degradation whereas the second stage is indicated the degradation of the PP at 400°C. However, in the presence of AS and TS, the thermal degradation temperatures of both phases of PP/CGF composites are relatively high (approximately 11.5°C and 14.9°C), indicating higher thermal stability than composites without silane. The maximum peak temperature increase may be highly related to the increased inorganic silane content on the CGF surface.

Table 3 Thermal degradation temperatures of virgin PP and its composites.

Sample	T_{onset} (°C)	$T_{25\%}$ (°C)	$T_{60\%}$ (°C)	Char residue at 600°C (wt%)
PP	262.3	395.3	429.1	5.1
PP/CGF	277.2	365.7	438.3	10.8
PP/ACGF	296.4	393.6	442.6	11.1
PP/ACGF/AS	303.2	399.5	444.5	11.8
PP/ACGF/TS	320.6	399.8	451.4	13.3

Notes: T_{onset}: initial decomposition temperature at which 5% weight loss occurred; $T_{25\%}$: the temperature at which 25% weight loss occurs; $T_{60\%}$: the temperature at which 60% weight loss occurs.

3.7 Differential scanning calorimetry (DSC)

The cooling and heating curves of virgin PP and PP/CGF composites with and without coupling agents were studied by DSC (Figure 10, a-d). Figure 10(a) displays the crystallization temperature (T_c) of neat PP was 116.5°C and the inclusion of 40 wt% CGF to neat PP increased T_c for composites without coupling agents by about 2.2°C. This may be owing to nucleation sites constructed in the existence of CGF. For PP/ACGF/AS and PP/ACGF/TS composites, T_c rises to 2.9-5.0°C, respectively, which further enhances the nucleation mechanism by coupling agents. The ester connection between PP and CGF may increase the nucleation of the PP matrix produced by the addition of AS and TS.

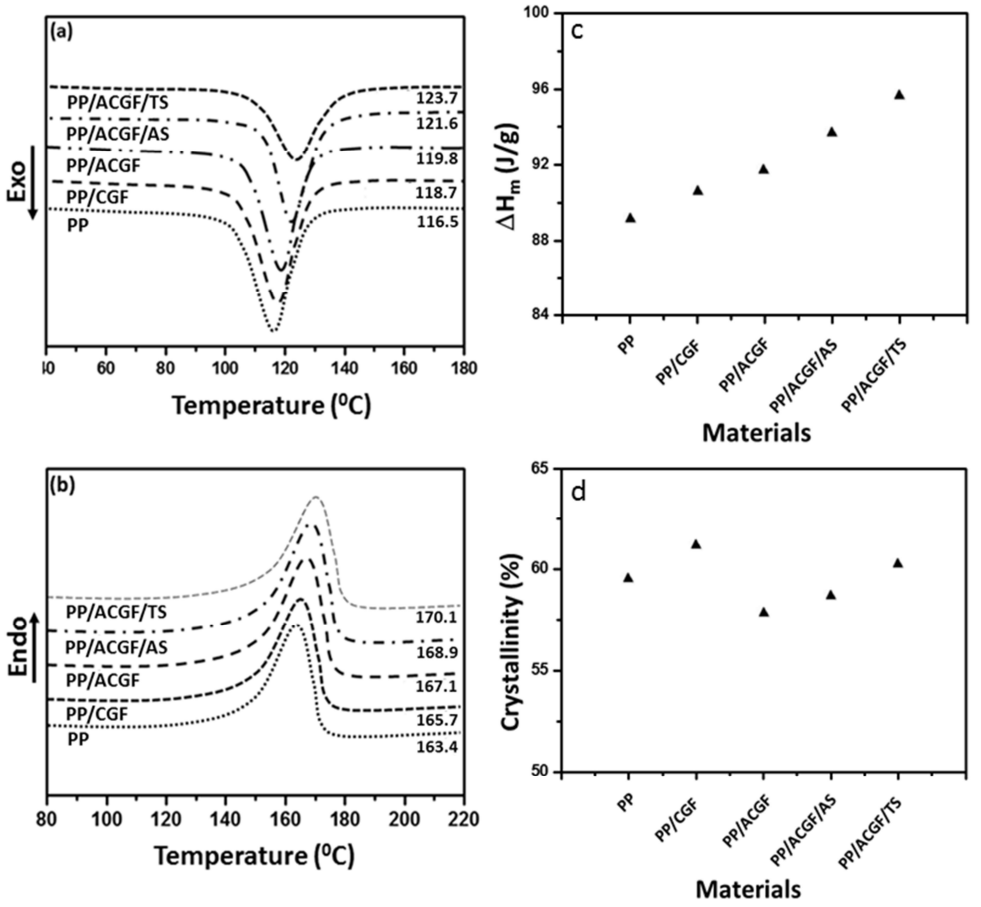

Figure 10 (a) DSC thermograms of PP/CGF, PP/ACGF, PP/ACGF/AS and PP/ACGF/TS composites: (a) cooling cycle, (b) heating cycle, (c) melting enthalpy, and (d) crystallization behavior.

The melting temperature (T_m) of virgin PP was 163.4°C (Figure 10, b). The inclusion of CGF (40 wt%) in virgin PP increased T_m by about 2.3°C. This is thought to be due to fiber-fiber interaction and fiber-polymer interaction, which contributes to the marginal increase in T_m of PP in PP/CGF composites. Furthermore, the inclusion of AS and TS in PP/CGF samples exhibited 3.2-4.4°C higher than in PP/CGF composites. T_m can be enhanced as compatibility between the two ingredients. It was found that the melting enthalpy (ΔH_m) of virgin PP was 89.5 J/g (Figure 10, c). The addition of CGF (40 wt%) to virgin PP enhanced the ΔH_m to 90.9°C. The addition of AS and TS in PP/CGF composites exhibited more ΔH_m than PP/CGF composites. These outcomes imply that composites with silane will melt, requiring greater vitality. TS provides better ΔH_m for PP/CGF composites than AS.

Figure 10(d) shows that the value of crystallinity (X_c) increased with the inclusion of CGF. Since CGF acts as the nucleation site of PP, so it increases the degree of crystallization and accelerates the crystallization rate. The reason for the decrease in X_c values of PP/ACGF/AS and PP/ACGF/TS composites is the increasing interaction between CGF and AS or TS, which hinders the crystallization phase of the matrix and decreases the degree of crystallization related to PP/CGF samples. Nevertheless, the inclusion of AS or TS to CGF increases the intermolecular interaction between PP and CGF. This seems to hinder the crystallization of the PP phase in AS and TS.

3.8 Water absorption (WA)

The WA quality results of PP/CGF, PP/ACGF, PP/ACGF/AS, and PP/ACGF/TS composites are presented in Figure 11 against CGF content as a function of water soaking time (24 hours). The immersion time and CGF loading are substantial issues, which impress the WA of the composites. After soaking the sample in water for 24 hours, the WA of PP/40 wt% CGF composites were 12% higher than PP/30 wt% CGF composites because of higher availability of cellulose -OH group which can absorb water. In contrast, PP/ACGF composite offered more WA (0.85%) than PP/ACGF/AS (0.68%) and PP/ACGF/AS (0.59%) composites, which were unable to eliminate the -OH groups on the surface of the CGFs. On the other hand, surface changes by silane resulted in an enhanced mechanical interlocking between CGF and PP and thereby WA was less for PP/ACGF/AS and PP/ACGF/TS composites.

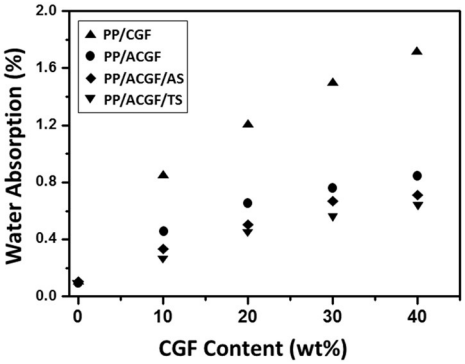

Figure 11 WA of PP/CGF, PP/ACGF, PP/ACGF/AS, and PP/ACGF/TS composites in different CGF contents.

4. Conclusions

In this study, the influences of chemical treatment (alkali and silane treatment) for CGF content on the basic properties of PP/CGF composites were examined. Based on research outcomes, conclusions can be drawn as follows:

Mechanical properties such as tensile modulus, impact strength, and hardness of PP/CGF composites were improved by increasing the amount of CGF in the optimum fiber content of 40 wt%. But the tensile strength was reduced to 40 wt% CGF content.

The mechanical and water desorption properties of PP/ACGF/AS and PP/ACGF/TS composites were higher than that of untreated composites.

SEM micrographs show an improvement in the interfacial CGF-PP adhesion of reinforced composites with alkali-pretreated silane-treated CGFs.

Addition of magnesium hydroxide to PP/ACGF/ AS and PP/ACGF/TS composites significantly reduced the combustion rate.

The thermal properties of PP/CGF composites were enhanced by the addition of AS, and TS. In contrast, the degree of crystallinity was reduced by adding AS, and TS.

Water absorption of treated composites was reduced compared to control composites.

Declaration of conflicting interests

The authors declared that they have no conflicts of interest in the research, authorship, and this article's publication.

References

1. Zaman H.U., Khan R.A. Improving the Physico-mechanical and Degradable Properties of Thermoplastic Polymer with Modified Starch Blend Composites for Food packaging Applications. Progress in Applied Science and Technology. 2021;11(3):1-8.
2. Zaman H.U., Beg M.D.H. Effect of Filler Starches on Mechanical, Thermal and Degradation Properties of Low-Density Polyethylene Composites. Progress in Applied Science and Technology. 2021;11(2):26-36.
3. Hassan M.M., Wagner M.H., Zaman H.U., Khan M.A. Physico-mechanical performance of hybrid betel nut (Areca catechu) short fiber/seaweed polypropylene composite. Journal of Natural Fibers. 2010;7(3):165-77.
4. Hassan M.M., Khan M.A. Effect of radiation pretreatment on photo-grafting of acrylamide on cellulose. Journal of Adhesion Science and Technology. 2009;23(2):247-57.
5. Hassan M.M., Wagner M.H., Zaman H.U., Khan M.A. Study on the performance of hybrid jute/betel nut fiber reinforced polypropylene composites. Journal of Adhesion Science and Technology. 2011;25(6-7):615-26.
6. Mohanty A., Misra M.A., Hinrichsen G. Biofibers, biodegradable polymers, and biocomposites: An overview. Macromolecular Materials and Engineering. 2000;276(1):1-24.
7. Zaman H.U., Beg M.D.H. Biodegradable Composites Manufactured from Low-Density Polyethylene and Thermoplastic Sago Starch: Preparation and Characterization. Progress in Applied Science and Technology. 2021;11(2):42-49.
8. Nordin M., Sakamoto K., Azhari H., Goda K., Okamoto M., Ito H., et al. Tensile and impact properties of pulverized oil palm fiber reinforced polypropylene composites: A comparison study with wood fiber reinforced polypropylene composites. Journal of Mechanical Engineering and Sciences. 2018;12(4):4191-202.
9. Latif R., Wakeel S., Zaman Khan N., Noor Siddiquee A., Lal Verma S., Akhtar Khan Z. Surface treatments of plant fibers and their effects on mechanical properties of fiber-reinforced composites: A review. Journal of Reinforced Plastics and Composites. 2019;38(1):15-30.
10. Zaman H.U., Khan M.A., Khan R.A., Beg D. A comparative study on the mechanical, degradation and interfacial properties of jute/LLDPE and jute/natural rubber composites. International Journal of Polymeric Materials. 2011;60(5):303-15.
11. Zaman H.U., Khan M.A., Khan R.A., Sharmin N. Effect of chemical modifications on the performance of biodegradable photocured coir fiber. Fibers and Polymers. 2011;12(6):727.
12. Zaman H.U., Khan M.A., Khan R.A., Mollah M., Pervin S., Al-Mamun M. A comparative study between gamma and UV radiation of jute fabrics/polypropylene composites: effect of starch. Journal of Reinforced Plastics and Composites. 2010;29(13):1930-39.
13. Zaman H.U., Beg M.D.H. Study on binary low-density polyethylene (LDPE)/thermoplastic sago starch (TPS) blend composites. Progress in Applied Science and Technology. 2021;11(1):53-65.
14. Velusamy K., Navaneethakrishnan P., Arungalai V.S., Saravana K.K., editors. Experimental investigations to evaluate the mechanical properties and behavior of raw and Alkali Treated king's crown (Calotropis Gigantea) fiber to be employed for fabricating fiber composite. Applied Mechanics and Materials; 2014: Trans Tech Publ.
15. Zaman H.U., Beg M. Preparation, structure, and properties of the coir fiber/polypropylene composites. Journal of Composite Materials. 2014;48(26):3293-301.

16. Ramesh M., Deepa C., Selvan M.T., Rajeshkumar L., Balaji D., Bhuvaneswari V. Mechanical and water absorption properties of Calotropis gigantea plant fibers reinforced polymer composites. Materials Today: Proceedings. 2021;46:3367-72.
17. Ramesh G., Subramanian K., Sathiyamurthy S., Prakash M. Calotropis Gigantea fiber-epoxy composites: Influence of fiber orientation on mechanical properties and thermal behavior. Journal of Natural Fibers. 2020:1-13.
18. Svensson N., Shishoo R., Gilchrist M. The tensile and flexural properties of textile composites. The Journal of The Textile Institute. 1998;89(4):635-46.
19. Park B.-D., Wi S.G., Lee K.H., Singh A.P., Yoon T.-H., Kim Y.S. Characterization of anatomical features and silica distribution in rice husk using microscopic and micro-analytical techniques. Biomass and Bioenergy. 2003;25(3):319-27.
20. Khan M.A., Khan R.A., Haydaruzzaman, Ghoshal S., Siddiky M., Saha M. Study on the physicomechanical properties of starch-treated jute yarn-reinforced polypropylene composites: effect of gamma radiation. Polymer-Plastics Technology and Engineering. 2009;48(5):542-48.
21. Zaman H.U., Khan R.A. Effect of fiber surface modifications on the properties of snake grass fiber reinforced polypropylene bio-composites. Journal of Adhesion Science and Technology. 2021:1-19.
22. Zaman H.U., Khan R.A. A Novel Strategy for Fabrication and Performance Evaluation of Bamboo/E-Glass Fiber-Reinforced Polypropylene Hybrid Composites. International Journal of Research. 2021;8(5):201-11.
23. Yang H.-S., Kim H.-J., Son J., Park H.-J., Lee B.-J., Hwang T.-S. Rice-husk flour filled polypropylene composites; mechanical and morphological study. Composite Structures. 2004;63(3-4):305-12.
24. Narendar R., Dasan K.P. Chemical treatments of coir pith: morphology, chemical composition, thermal and water retention behavior. Composites Part B: Engineering. 2014;56:770-79.
25. Widnyana A., Rian I.G., Surata I.W., Nindhia T.G.T. Tensile Properties of coconut Coir single fiber with alkali treatment and reinforcement effect on unsaturated polyester polymer. Materials Today: Proceedings. 2020;22:300-05.
26. Singha A.S., Thakur V.K. Morphological, thermal, and physicochemical characterization of surface-modified pinus fibers. International Journal of Polymer Analysis and Characterization. 2009;14(3):271-89.
27. Zaman H.U., Khan M.A., Akter N., Ghoshal S., Khan R.A. Role of gamma radiation and EGDMA on the physicomechanical properties of jute fabrics/polypropylene composites. Polymer Composites. 2011;32(11):1888-94.
28. Zaman H.U., Khan M.A., Khan R.A., Ghoshal S. Effect of ionizing and non-ionizing preirradiations on physicomechanical properties of coir fiber grafting with methylacrylate. Fibers and Polymers. 2012;13(5):593-99.
29. Masudul Hassan M., Islam M.R., Khan M.A. Improvement of physicomechanical properties of jute yarn by photografting with 3-(trimethoxysilyl) propylmethacrylate. Journal of Adhesion Science and Technology. 2003;17(5):737-50.
30. Khan M.A., Drzal L.T. Characterization of 2-hydroxyethyl methacrylate (HEMA)-treated jute surface cured by UV radiation. Journal of Adhesion Science and Technology. 2004;18(3):381-93.
31. ASTM Standard D 785-98 S.t.m.f.R.h.o.p.a.e.i.m., Annual Book of ASTM Standards, Vol. 08.01.2002.
32. Salon M.-C.B., Abdelmouleh M., Boufi S., Belgacem M.N., Gandini A. Silane adsorption onto cellulose fibers: Hydrolysis and condensation reactions. J Colloid Interface Science. 2005;289(1):249-61.
33. Haydaruzzaman, Khan A., Hossain M., Khan M.A., Khan R.A. Mechanical properties of the coir fiber-reinforced polypropylene composites: effect of the incorporation of jute fiber. Journal of Composite Materials. 2010;44(4):401-16.

34. Aziz S.H., Ansell M.P. The effect of alkalization and fiber alignment on the mechanical and thermal properties of kenaf and hemp bast fiber composites: Part 1-polyester resin matrix. Composites Science and Technology. 2004;64(9):1219-30.
35. Joseph K ML T.R., et al. . Natural fiber-reinforced thermoplastic composites. Natural Polymers and Agrofibers Bases Composites. Embra Instr Agro, Sao Carlos. 13560-970 SP, Brazil 2000; 2000: 159-201.
36. Jamil M.S., Ahmad I., Abdullah I. Effects of rice husk filler on the mechanical and thermal properties of liquid natural rubber compatibilized high-density polyethylene/natural rubber blends. Journal of Polymer Research. 2006;13(4):315-21.
37. Thwe M.M., Liao K. Effects of environmental aging on the mechanical properties of bamboo–glass fiber reinforced polymer matrix hybrid composites. Composites Part A: Applied Science and Manufacturing. 2002;33(1):43-52.
38. Zaman H.U., Beg M. Effect of coir fiber content and compatibilizer on the properties of unidirectional coir fiber/polypropylene composites. Fibers and Polymers. 2014;15(4):831-38.
39. Titelman G., Gonen Y., Keidar Y., Bron S. Discolouration of polypropylene-based compounds containing magnesium hydroxide. Polymer Degradation and Stability. 2002;77(2):345-52.
40. Rosa M.F., Chiou B.-s., Medeiros E.S., Wood D.F., Williams T.G., Mattoso L.H., et al. Effect of fiber treatments on tensile and thermal properties of starch/ethylene vinyl alcohol copolymers/coir biocomposites. Bioresource Technology. 2009;100(21):5196-202.

